ELSEVIER

Journal of Atmospheric and Solar-Terrestrial Physics 69 (2007) 419–430

Journal of ATMOSPHERIC AND SOLAR-TERRESTRIAL PHYSICS

www.elsevier.com/locate/jastp

Diurnal and seasonal variability of TKE dissipation rate in the ABL over a tropical station using UHF wind profiler

Madhu Chandra Reddy Kalapureddy[a,*], K. Kishore Kumar[b], V. Sivakumar[c], A.K. Ghosh[d], A.R. Jain[e], K. Krishna Reddy[f]

[a]*Indian Institute of Tropical Meteorology, Pashan, Pune, India*
[b]*Space Physics Laboratory, Trivandram, India*
[c]*National Laser Centre, Council for Scientific and Industrial Research (CSIR), Pretoria, South Africa*
[d]*Satish Dhawan Space Center, Shriharikota, India*
[e]*National Physical Laboratory, New Delhi, India*
[f]*Frontier Observational Research System for Global Change, Yokohama, Japan*

Received 10 March 2006; received in revised form 30 October 2006; accepted 30 October 2006
Available online 16 January 2007

Abstract

This paper presents the diurnal and seasonal variation of Turbulence Kinetic Energy (TKE) dissipation rate (ε) in the Atmospheric Boundary-Layer (ABL) over a tropical station, Gadanki (13.5° N, 79.2° E) in India. Doppler spectral width measurements made by Lower Atmospheric Wind Profiler (LAWP) operating at 1357 MHz are utilized to estimate ε in the height region of 0.5–4.0 km on clear air days. Various non-turbulent spectral broadenings are calculated and separated out from the observed spectral width before estimating ε. It is found that in the lower tropospheric height region ε is in the range from $10^{-5.0}$ to $10^{-1.0}\,m^2\,s^{-3}$. ε showed significant diurnal variation in the boundary-layer. The larger values of ε, $10^{-2.7}\,m^2\,s^{-3}$, are noted to be associated with the Convective Boundary-Layer (CBL). The parameter ε is also showing significant seasonal variation. In summer and monsoon seasons the boundary-layer depths are observed up to a height of ~4.0 km while the same are confined to below 2.0 km in post-monsoon and winter seasons.

Keywords: Atmospheric boundary-layer (3307); Turbulence energy dissipation rate (4490); Radar Doppler spectral width (1120); UHF wind profiler (6969)

1. Introduction

The Convective Boundary-Layer (CBL) is considered to be a well-mixed layer due to the presence of strong atmospheric turbulence. Turbulence is an important transport process in the boundary layer. It contributes dissipation and diffusion of heat and momentum in the atmosphere. Turbulence also influences the diffusion of pollutants from near Earth's surface to the higher heights. So, a comprehensive knowledge of the turbulence parameters is essential for several applications in numerical, chemical, and energy budget modeling and also helps in thorough understanding of the dynamics of the lower atmosphere.

*Corresponding author. Tel.: +91 20 25893600; fax: +91 20 25893825.
E-mail address: kalapureddy1@gmail.com (M.C.R. Kalapureddy).

1364-6826/$ - see front matter © 2006 Elsevier Ltd. All rights reserved.
doi:10.1016/j.jastp.2006.10.016

The UHF wind profilers are better suited for boundary-layer observations (Ecklund et al., 1988; Rogers et al., 1993; Gossard et al., 1998). One such UHF radar, known as Lower Atmospheric Wind Profiler (LAWP), is located at Gadanki (13.5° N, 79.2° E) to support the research on the boundary layer and the precipitation. Various features of LAWP at Gadanki are given by Krishna Reddy et al. (2001). Many researchers have examined the possibility of deducing the turbulence parameters like eddy dissipation rate (ε) and eddy diffusivity (K_h) from the observed Doppler spectrum of the wind profiler (e.g., Gage and Balsley, 1978; Gossard, 1990; Gage, 1990; Narayana Rao et al., 2001; Satheesan and Krishna Murthy, 2002). One of the limitations of UHF radar for the studies on atmospheric turbulence is its sensitivity to the hydrometeors. It is, therefore, necessary to choose clear air days for estimating the turbulence parameters from the UHF radar observations. Spectral width, obtained from the radar Doppler spectrum, has been extensively used in many studies on turbulence (e.g., Frisch and Clifford, 1974; Sato and Woodman, 1982; Doviak and Zrnic, 1984; Hocking, 1983, 1985; Fukao et al., 1994; Jain et al., 1995; Nastrom and Eaton, 1997; Narayana Rao et al., 1997; Hermawan and Tsuda, 1999; White et al., 1999; Furumoto and Tsuda, 2001; Sandra Jocoby-Koaly et al., 2002).

The purpose of the present study is to estimate ε by a suitable method applicable for radar-probed CBL and understand the diurnal and seasonal variability of ε. This is the first time an attempt is made, near tropics, to understand high-resolution diurnal and seasonal features of turbulence and wind in the boundary-layer region.

2. System description

LAWP is coherent, pulsed Doppler radar with an effective peak power aperture product of about $1.2 \times 10^4\,\mathrm{W\,m^{-2}}$. This radar can detect the backscattered echoes from approximately 11 cm irregularities. The major specifications of the system are given in Table 1. LAWP makes use of a phased array of 3.8×3.8 m organized in four quadrants, each having an array of 12×12 circular conducting patch antenna elements for transmission and reception. The power distribution across the array is tapered to obtain better side-lobe suppression. The LAWP system has been configured to operate in Doppler Beam Swinging (DBS) mode. The antenna beam can be positioned, through electrical phase switching, at any of three fixed orientations, viz., Zenith, 15° from Zenith to both East and North directions. The transmitter frequency is 1357 MHz and the maximum receiver gain is 120 dB. The parameterization of the Doppler signal spectrum data of LAWP, in the present study, follows closely the procedure adopted at the Poker Flat radar (Riddle, 1983). The three lower-order spectral moments, the signal strength, the weighted mean Doppler shift, and the spectral width, are computed then through numerical integration using the expressions given by Woodman (1985). The mean Doppler shift provides a direct measure of the radial velocity of scattering refractive irregularities which act as tracers of the background wind. It is straightforward to derive the three components of the wind vector from the measurements taken at a minimum of three non-coplanar beam positions. Further details on analysis procedure can be found in Anandan et al. (2005).

State-of-art MST radar is collocated with LAWP at Gadanki site. This MST radar operates at VHF (53 MHz) and has a peak power aperture product of $3 \times 10^{10}\,\mathrm{W\,m^{-2}}$ (Rao et al., 1995). Three

Table 1
LAWP System and Experimental Specifications

Parameter	Specifications
Location	Gadanki (13.5° N, 79.2° E)
Antenna (Phased Array)	3.8×3.8 m
Frequency (f)	1357.5 MHz
Radar wave length (λ_R)	0.22 m
Transmitted power (P_t)	1000 W
Effective Aperture (A_e)	$10\,\mathrm{m^2}$
Beam width	4°
No. of beams	3 (Zenith, 15° down to North and East)
Gain (G)	33 dB
Receive band width (B_N)	1.58×10^6 Hz
Receiver path loss (α_r)	−4 dB
Transmitter path loss (α_t)	−0.5 dB
Cosmic temperature (T_c)	10 K
Receiver temperature (T_r)	107 K
Maximum duty	0.05
Pulse width	1 μs
Inter pulse period	70 μs
Range resolution (δ_r)	150 m
Coherent integration (N_C)	100
No. of FFT points	128
Observational range	0.3–9.25 km
Incoherent integration	100
Beam Dwell time	90 s
Boltzmann constant (k)	$1.38 \times 10^{-23}\,\mathrm{J\,K^{-1}}$

components of wind (U, V and W) can be measured using this radar from 1.5 km onwards by transmitting RF pulses of 1 μs width. Wind measurements using simultaneous LAWP and MST radar observations are compared in the overlapping region. It has shown good agreement between the measurements with correlation coefficients of 0.94, 0.80, and 0.78 for zonal (U), meridional (V), and vertical (W) wind components, respectively (Madhu C Reddy et al., 2000).

3. Method of estimation of eddy dissipation rate

The Turbulence Kinetic Energy (TKE) plays a vital role in determining the atmospheric dynamics and coupling. The TKE depends on TKE dissipation rate or eddy dissipation rate (ε). The parameter ε gives the turbulence in the velocity field and it is one of the fundamental parameters used to determine the turbulence characteristics. It represents the rate of energy cascading to smaller eddy until the energy is converted into heat due to the presence of viscous force.

In the present study, a method that makes use of the radar signal spectral width, developed due to successive and progressive efforts of Sloss and Atlas (1968), Frisch and Clifford (1974), Gossard et al. (1998), and White et al. (1999) is used. This method has been established for marking CBL heights and the estimated ε values compare well with *in situ* observations (Sandra Jocoby-Koaly et al., 2002). The main assumptions in this method are isotropic and homogeneous turbulence, a Gaussian antenna symmetric illumination function, and a Gaussian radial response of the receiver. The turbulent variance is related to ε by the following equation given by White et al. (1999).

$$\varepsilon = \sigma_{\text{turb}}^3 (4\pi/A)^{3/2} J^{-3/2}, \tag{1}$$

where σ_{turb} is spectral width due to turbulence, A is a 3-D Kolmogorov constant ranges from 1.53 to 1.68 (Gossard and Strauch, 1983) and the term J is given by

$$J = 12\Gamma(2/3) \int\int (\sin^3\varphi)(b^2\cos^2\varphi + a^2\sin^2\varphi + (L^2/12)\sin^2\varphi\cos^2\phi)^{1/3} \mathrm{d}\varphi\,\mathrm{d}\phi, \tag{2}$$

where Γ is Gamma function. L is the product of the mean wind speed and the Doppler time series duration. The double integration is taken between 0 and $\pi/2$ for both spherical coordinates φ and ϕ. J has to be solved numerically with an estimate of the mean wind speed provided by the profiler. The parameter $a = r\theta/4\sqrt{\ln 2}$, here r and θ are range and one-way half power beam width, respectively. The parameter $b = \alpha h$, here h is pulse length and the proportionality constant α is equal to $1/8\sqrt{\ln 2}$ for an infinite response of the receiver. The Gaussian response of LAWP receiver is 0.625 MHz. More information on theoretical background of Eqs. (1) and (2) can be found in the works of Frisch and Clifford (1974), White et al. (1999) and Sandra Jocoby-Koaly et al. (2002). One of the advantages of this method is that sole radar data is sufficient and no radiosonde data is needed for computing ε.

The turbulence refractivity structure parameter C_n^2 is also computed by using the following equation (Jain et al., 1995; Ghosh et al., 2003):

$$C_n^2 = \frac{32(\ln 2) K B_N (\alpha_r T_c + T_r) \lambda^{1/3} r^2}{0.38 \alpha_t \alpha_t A_e \delta_r N_B N_C P_t} (\text{SNR}) \tag{3}$$

and the symbols details are given in Table 1. Eq. (3) can be rewritten as

$$C_n^2 = k r^2 (\text{SNR}) \tag{4}$$

where k is the radar constant. For LAWP system, $k \approx 6.98 \times 10^{-16}$.

The off-zenith beams observed mean radar signal spectral width (σ_{obs}) contains the contributions due to turbulent and non-turbulent processes. Some of the non-turbulent processes are the beam broadening (σ_{beam}^2), shear broadening (σ_{shear}^2), and the transience (σ_{trans}^2) (Fukao et al., 1994; Hocking, 1985; Nastrom, 1997). This can modify the shape of the observed radar spectrum. In order to estimate the actual spectral width (σ_{turb}) from turbulence alone, it is essential to remove the non-turbulent contaminations from the observed spectral width (i.e. $\sigma_{\text{turb}}^2 = \sigma_{\text{obs}}^2 - \sigma_{\text{shear}}^2 - \sigma_{\text{beam}}^2 - \sigma_{\text{trans}}^2$). When turbulence is weak this removal may occasionally lead to negative values (Hocking, 1988). Therefore, only positive values of σ_{turb}^2 are considered for present study. The measurement of the vertical spectral width, which is less affected by the large-scale broadening factor, has not been considered for this study due to the possible modification of vertical spectral width after ground clutter removal (Sandra Jocoby-Koaly et al., 2002).

The difference in radial wind velocity at different parts within a finite beam width leads to the broadening of the observed radar signal spectrum and is known as beam broadening effect (Nastrom,

1997; Hocking, 1990). It can be quantified as

$$\sigma_{\text{beam}} \approx (d_{1/2})|\overline{V_{\text{h}}}|, \tag{5}$$

where $\delta_{1/2} \approx 0.024$ radians ($=1.4^{\circ}$) for LAWP and it is the half-power half width of the effective (two way) radar beam, and $\overline{V_{\text{h}}}$ is the background horizontal mean wind speed.

The shear broadening to the spectral width arises due to vertical gradient of horizontal wind within the sample volume (due to finite pulse width). For a known horizontal wind shear, this shear broadening can be expressed (Fukao et al., 1994; Nastrom, 1997) as

$$\sigma_{\text{shear}} \approx \frac{1}{2}\left|\frac{\partial \bar{v}_{\text{h}}}{\partial z}\right|\Delta z \sin 15^{\circ}, \tag{6}$$

where Δz is sampled volume which is 150 m and radar beam off-zenith angle is 15°.

The transient broadening effect is caused by the wind variations during the time period used for incoherent integration (see for more details Hocking, 1985, 1988). If $\bar{u}'_{2\tau}$ is the variance of the radial velocity for an integration interval τ (Hocking, 1988), then the transient contamination, due to transient atmospheric motions, is estimated by

$$\sigma^2_{\text{trans}} \approx 4(\bar{u}'_{2\tau})^2. \tag{7}$$

The effect of above corrections on the observed spectral width and its significance can be seen from Fig. 1. Height profiles of spectral width variance (σ^2) between observed spectral width (σ_{obs}) and corrected spectral width (σ_{turb}) show significant (trivial) difference on 27 July 1999 (10 August 1999). It has been observed, not shown in figure, that strong (normal) wind speed on 27 July 1999 (10 August 1999) is in the range 15–20 m s^{-1} (6–8 m s^{-1}) in the height region 0.5–4.0 km. It has also been observed that the corrections are significant whenever strong wind and associated sharp gradients exist.

4. Results and discussion

LAWP has been operated daily round-the-clock as per the experimental specifications given in Table 1. The high-resolution (150 m in height and 10 min in time) data collected during different seasons of 1999–2000 have been used to study diurnal and

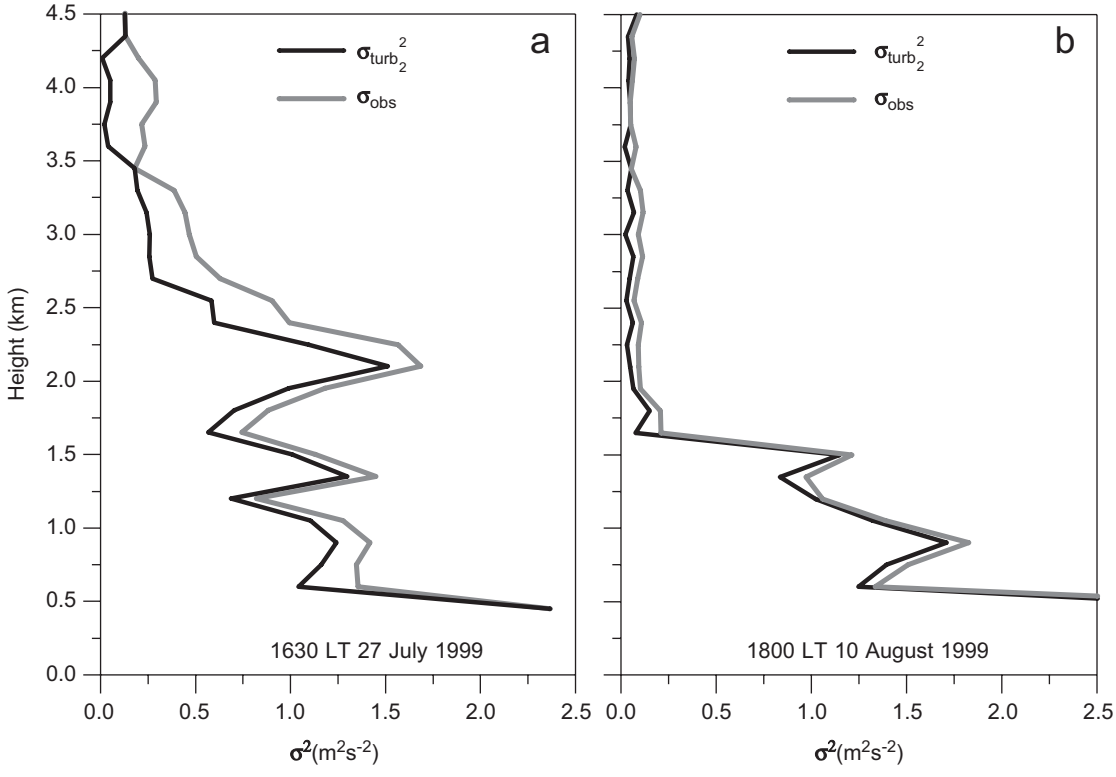

Fig. 1. Height profiles of observed and corrected spectral width square (σ^2_{obs} and σ^2_{turb}) on two typical days viz., 27 July 1999 and 10 August 1999.

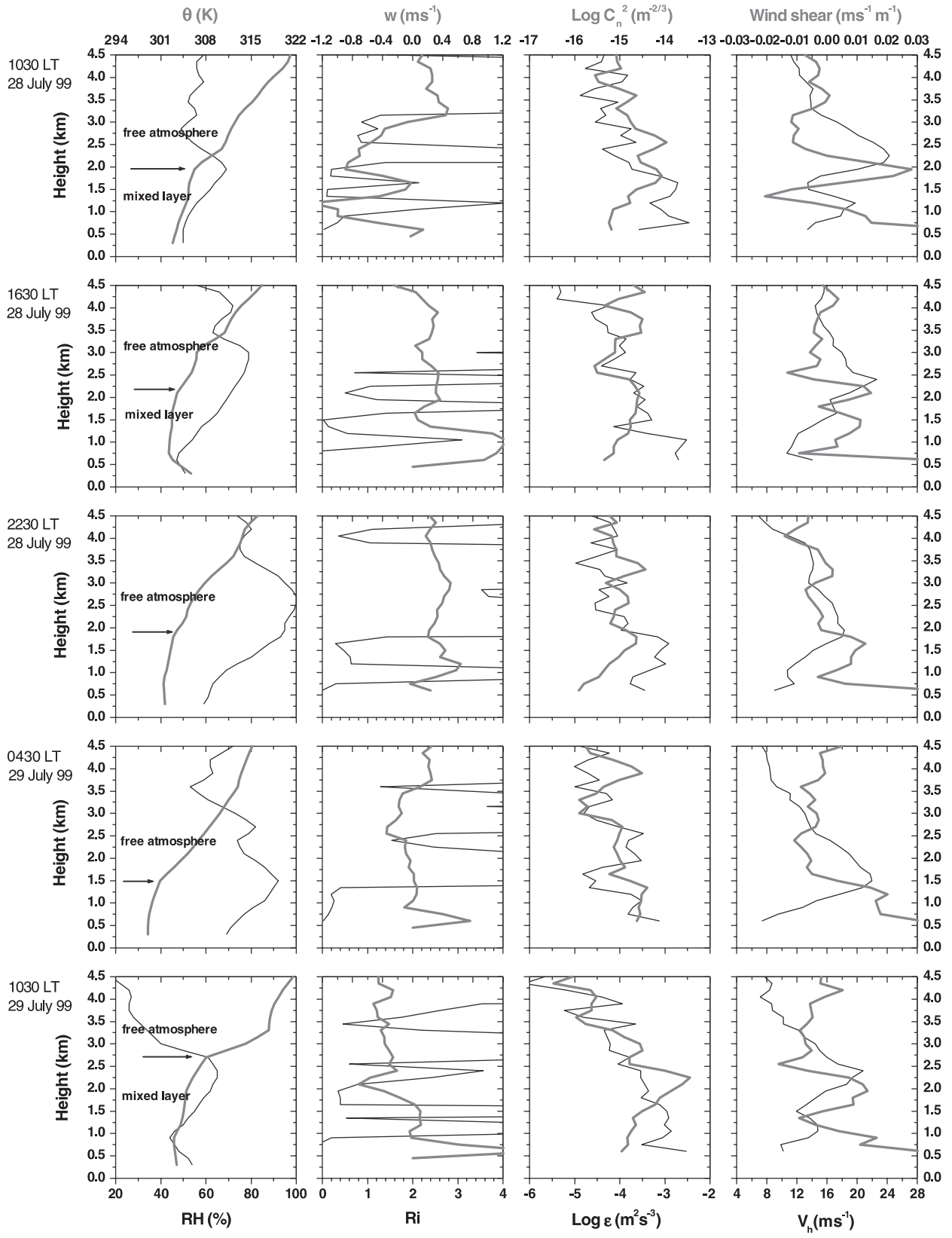

Fig. 2. Height profiles of various parameters for every 6 h interval from 1030 LT on 28 July 1999 to 1030 LT on 29 July 1999 can be seen from top to bottom row panels, respectively. Arrow (left most graphs) indicates the top of mixed layer.

seasonal variations of boundary-layer features. All the data selected for the present study are free from precipitation. The simultaneous LAWP and radiosonde observations carried out at Gadanki have been utilized to verify the diurnal variability of boundary-layer depth shown by LAWP. The height profiles of various ABL dynamical and meteorological parameters, derived from simultaneous LAWP and radiosonde observations on 28 and 29 July 1999 are shown in Fig. 2. In this figure, each horizontal

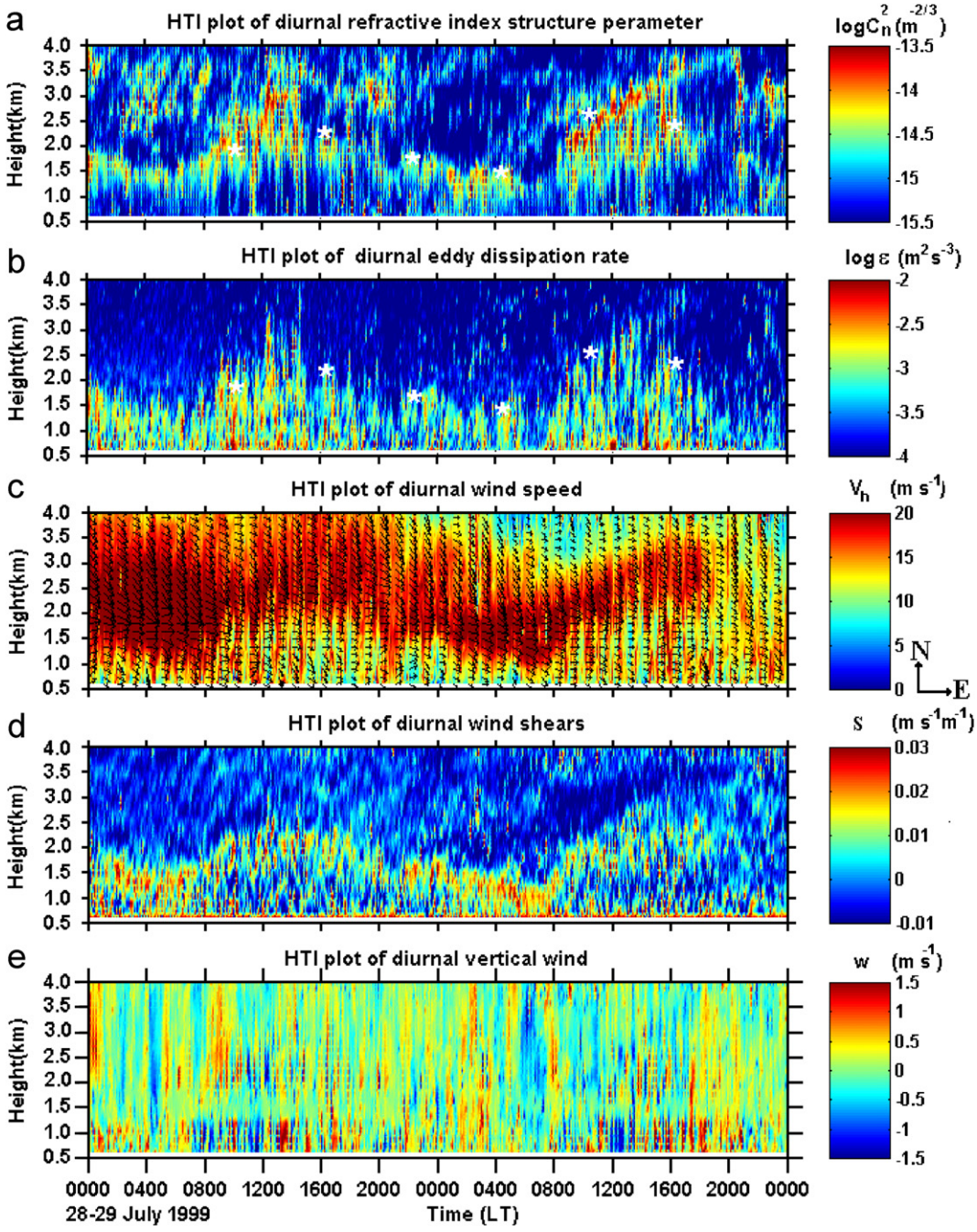

Fig. 3. Height-Time-Intensity (HTI) diurnal plots of (a) refractive index structure parameter (b) eddy dissipation rate (c) wind speed (d) wind shear and (e) vertical wind for two diurnal cycles i.e. for 28 and 29 July 1999. The symbol asterisk represents the boundary-layer top found from low-level inversion shown by radiosonde data (see Fig. 2).

panel corresponds to particular time of radiosonde launch during 1030 LT of 28 July 1999–1030 LT of 29 July 1999, respectively with an observational interval of every 6 h. The height profiles of vertical wind (w), C_n^2, ε, horizontal wind speed (V_h), and vertical shear of the horizontal wind (S) are computed using the LAWP measurements averaged over 20 min around radiosonde launch time. The radiosonde-measured parameters are used to compute potential temperature (θ) and Richardson Number ($Ri = N^2/S^2$; where N^2 is stability parameter). The sharp gradient in height profile of θ (gray line in 1st column panel) can be used to differentiate the top of the boundary-layer and the free atmosphere (Angevine et al., 1994). The turbulence parameters C_n^2 and ε (gray and black line in 3rd column panel) show significant peaks near around the top of the boundary layer as pointed out by θ profile. This feature is utilized to estimate boundary-layer depth from sole radar measurements. Such altitudes, where Ri value is less than one, represent the regions where turbulent layers are likely to be present (Atlas et al., 1968). This can be observed as small peaks in ε around those levels. The background wind speed and associated shears can be seen in right most column panels. It can be noticed that the core height of low-level jet, just above the boundary layer, is varying with respect to time. Strong shears are noticed on either side of jet core. From Fig. 2, it is also noted that ε shows sharp decrease above the boundary-layer region. These 2 days i.e. 28 and 29 July 1999 represent the typical days for monsoon at this tropical station.

4.1. HTI diurnal maps of C_n^2, ε, and other dynamical parameters

It is well known that either radar reflectivity or C_n^2 can be used to identify the CBL top or CBL depth (Angevine et al., 1994; Sandra Jocoby-Koaly et al., 2002). The evolution of CBL, on 28 and 29 July 1999, can be seen clearly as an elevated layer of enhanced C_n^2 in Fig. 3(a) as Height-Time-Intensity (HTI) map. On these two days CBL reached as high as ~4.0 km during afternoon hours at the observational site, Gadanki, as it is expected in the tropics but it is near 1 km less compared to the boundary-layer depth reported for equatorial site, Indonesia (Hashiguchi et al., 1996). The symbol asterisk on the figure indicates the depth of CBL obtained from the low-level temperature inversion shown by radiosonde observations. Fig. 3(b) shows higher ε values in the boundary layer, $10^{-2.5}\,m^2\,s^{-3}$, during the noontime. It can also be observed that there is sharp decline in ε values above the boundary layer. The contrasting feature between Fig. 3(a) and (b) emphasizes the basic nature and significant difference in radar observed parameters viz., radar reflectivity and spectral width. The sharp increase in C_n^2 confined to top of the boundary layer is an indication of sharp change in the atmospheric refractivity caused due to the distinct gradient in temperature and humidity at the top of ABL. The

Table 2
Details of LAWP data used in exploring the seasonal features of boundary-layer turbulence

Sl. No.	Season	Month & Year	Date(s)	Data time gaps
I	Monsoon	June 1999 July 1999 August 1999 September 1999	03,11,18,25, and 28 02,10,18,26, and 28 02,13,19,20, and 31 02,04,10,19, and 21	Nil
II	Post-monsoon	October 1999 November 1999 December 1999	04,16,17,21, and 25 06,11,12,23, and 24 05,10,15,25, and 30	Nil
III	Winter	January 2000 February 2000	05,07,09,17, and 26 02,03,07,08,17, and 29	02 Feb'00- 0117-0335 03 Feb'00- 2025-2230 07 Feb'00- 1815-2030 08 Feb'00- 0317-0540 17 Feb'00- 1740-1810
IV	Summer	March 2000 April 2000 May 2000	01,02,03,20, and 28 05,10,11,18, and 19 05,07,12,17, and 21	05 Apr'00- 0800-0959 10 Apr'00- 0800-0859 18 Apr'00- 0820-0910

sharp decrease in ε above the boundary layer indicates the diminishing of turbulent eddies of sizes comparable to half of radar wavelength above the boundary-layer. Background wind during this period shows low-level jet feature, at around 1.5 km, with wind of order 20 m s^{-1}, which is a well-known phenomenon observed over southern India during the summer monsoon season (Joseph and Raman, 1966) and can be seen from Fig. 3(c). The strong wind shear associated with the jet can be noticed from Fig. 3(d). The vertical wind in Fig. 3(e) shows episode of updrafts and downdrafts in the CBL. A strong clutter noticed at 1.5 km range bin in the vertical beam is a reason of distraction of features at that height.

Continuous high-resolution observations of LAWP during 1999–2000 have been utilized to study the seasonal variation of ε in the CBL. The observations are divided into four seasons viz., summer (March–May), monsoon (June–September), post-monsoon (October–December), and winter (January and February). Radar observations are

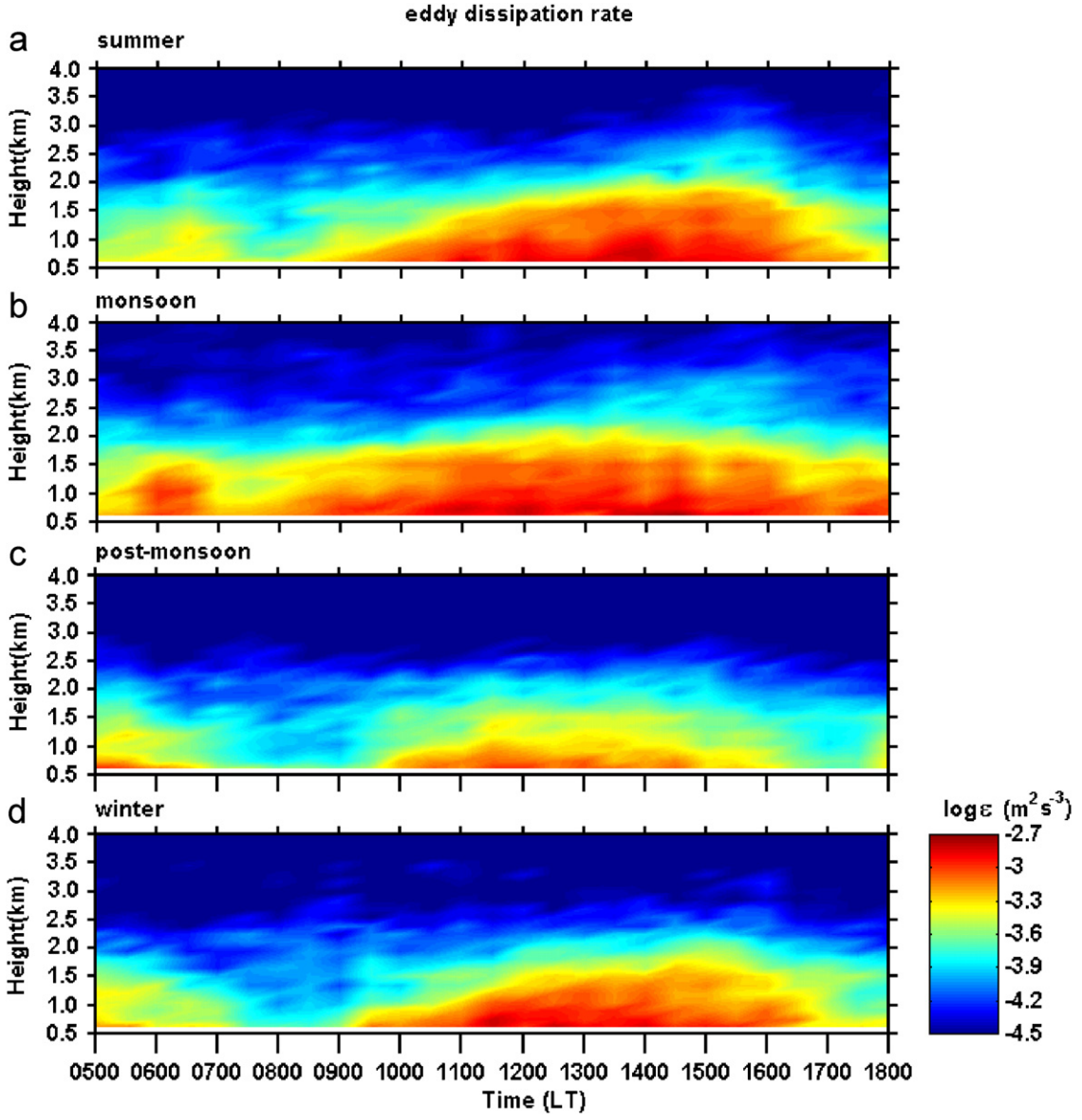

Fig. 4. Height-Time-Intensity (HTI) maps for the mean diurnal variation of eddy dissipation rate for seasons (a) Summer, (b) Monsoon, (c) Post-monsoon, and (d) Winter.

fairly continuous except during power failure or radar maintenance period. Moreover, due to the constraints such as clear air condition and nearly continuous quality data in a day to explore diurnal feature, a rational five minimum, fairly continuous, clear air diurnal days are chosen for each month. Details on data used are given in Table 2. The mean seasonal diurnal evolution of ε and background winds (V_h and w) have been obtained by averaging out respective mean half hourly values of all days in that season and can be seen in Figs. 4 and 5. Further, as the method used for estimating ε is essentially for CBL, the period 0500–1800 LT has been chosen for exploring the aggregate ε diurnal features for various seasons. All seasons show strong diurnal feature, exceptional to monsoon where the maximum boundary-layer depths are almost maintained with little variability in between ~0800 LT and ~1800 LT. In the monsoon season, the characteristic strong convective activity with water vapor loaded cross equatorial westerly wind (Joseph and Sijikumar, 2004) over south India could be the reason for the unique diurnal feature in monsoon. The growth of the monsoon CBL is very rapid and maximum mean boundary-layer depth is ~3 km, whereas, it is as high as ~4 km on an individual day (see Fig. 3). Monsoon mean winds are high (~15 m s^{-1}) and northwesterly in direction associated with low-level jet. Vertical winds in monsoon show low-level predominant updrafts, which aid in pumping more moisture into the free atmosphere. All seasons, except monsoon, show predominant easterly wind and subsidence in the CBL and it can be seen, respectively from wind speed and vertical wind panels of Fig. 5a, c and d. Summer and winter seasons show more or less similar diurnal features viz., mean boundary-layer depths of around 2.0 km and northeasterly wind speeds of order ~10 and ~6 m s^{-1}, respectively. During post-monsoon season the boundary-layer activity is weak and maximum depth is well below 2.0 km. Winds in this season are northeasterly of the order of 10 m s^{-1} in the CBL and are benign above it. From Fig. 5, it can be understood that during post-monsoon and winter seasons, the stronger eddy dissipation rate values, $10^{-2.7}$ m^2 s^{-3}, almost confined below ~1 km, whereas during monsoon stronger values extended up to 1.5 km. In the post-monsoon season, due to preceding continuous rains in monsoon, the essentially cool atmosphere and ocean around India and wet surface are unfavorable for convective activity and vigorous turbulence. Moreover, the trade wind inversion observed (not shown) around 2.3 km might be the reason to have such weak turbulent eddy dissipation rates and consequent thin boundary-layer depth during this season. From dry winter season, the boundary-layer eddy dissipation rate shows a gradual enhancement and leads to further increase in boundary-layer depth and becomes the strongest in monsoon season. Thereafter a sudden fall can be seen in the post-monsoon season. On the whole, the values of ε in the lower troposphere region are in the range from $10^{-5.0}$ to $10^{-1.0}$ m^2 s^{-3} and are comparable with the values reported by Cohn (1995), Hocking and Mu (1997), and Sandra Jocoby-Koaly et al. (2002). It can be noticed from Fig. 4 that, in general, boundary-layer depth starts evolving at around ~0900 LT and mean maximum depth confined in between 1430 and 1530 LT, and a sharp fall in boundary-layer depths can be seen around 1700 LT. It is evident that the ε values, in particular, are high within the CBL region. The presented high-resolution observations are first of its kind from tropical India, revealing the clear seasonal and diurnal features of ε, V_h and w in the boundary layer.

5. Conclusions

In the present paper, an attempt is made to understand the diurnal and seasonal variations of ε in the tropical convective boundary layer along with other background atmospheric parameters. The radar signal spectral width is used for the estimation of ε, using a method applicable for the convective boundary layer. To make use of this method the observed radar signal spectral width is corrected for contaminations arising due to various non-turbulent effects. It has been noticed that the ε values are very large in the CBL. In summer and monsoon seasons the large values of ε, $10^{-2.7}$ m^2 s^{-3}, are observed up to a height of ~1.5 km whereas the same is confined to a height of 1.0 km in post-monsoon and winter season. Further strongest and weakest ε values in the CBL are observed during monsoon and post-monsoon seasons, respectively. It is also observed that ε shows pronounced diurnal variability in the CBL in almost of all seasons. The mean ε shows large values in the boundary layer as compared to free atmosphere. Wind speeds are easterly in all seasons except monsoon. Monsoon wind speeds show westerly Jet feature at around 1.5 km. The vertical wind shows predominant subsidence in CBL in all the seasons except

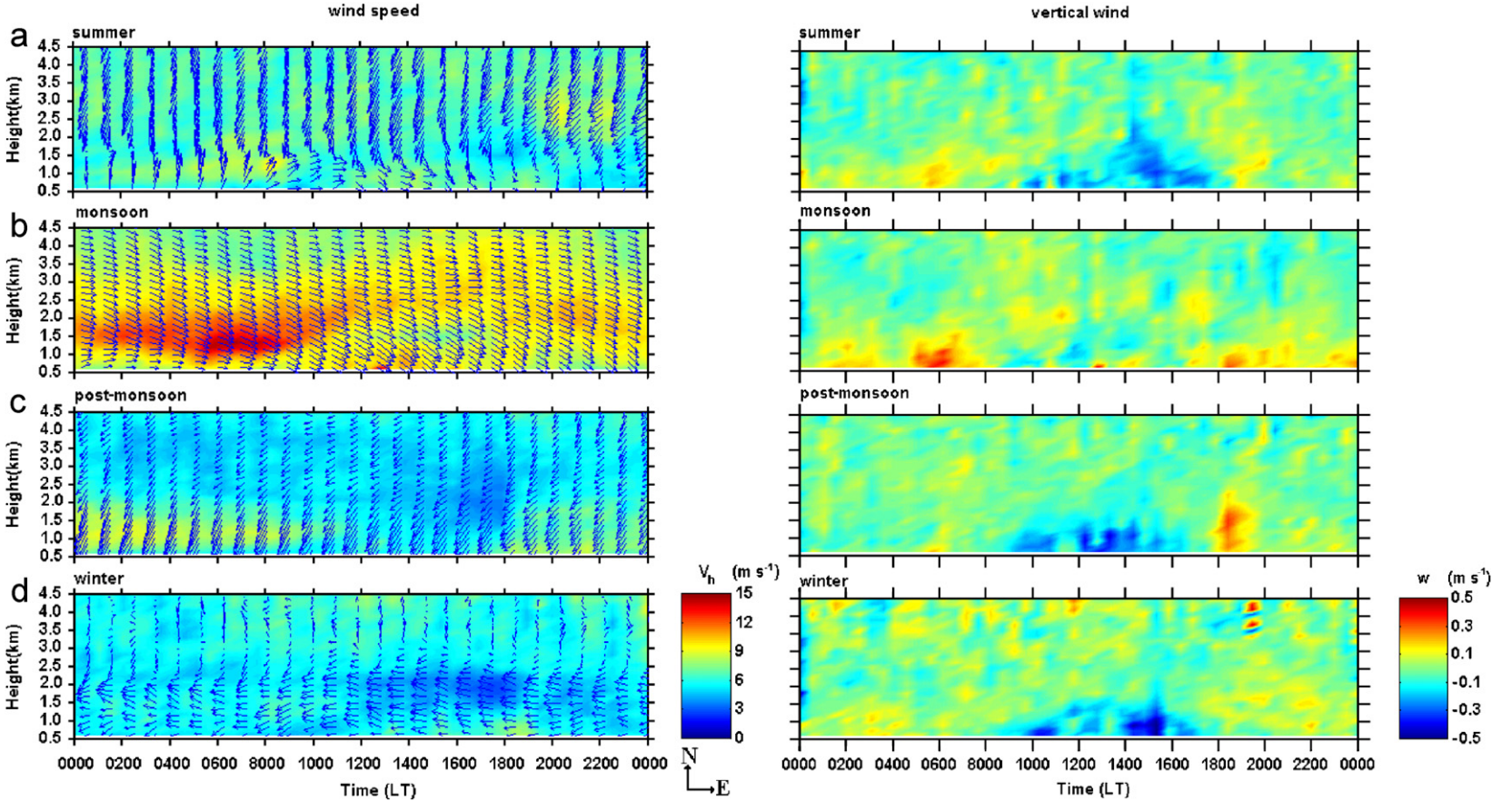

Fig. 5. Height-Time-Intensity (HTI) maps for the mean diurnal variation of wind speed (left side) and vertical wind (right side) for seasons (a) Summer, (b) Monsoon, (c) Post-monsoon, and (d) Winter.

monsoon where updrafts are prominent. Hence, the method used, solely based on radar returns, in this work is worthwhile for estimating TKE dissipation rates in the ABL.

Acknowledgments

The National Atmospheric Research Laboratory (NARL) is operated by Department of Space (DOS), Government of India. The LAWP system is established at NARL under a joint research project between MOPT/CRL, Japan, and DOS/NARL, India. Authors are thankful to NARL colleagues, for their every support. We are thankful to the India Meteorological Department (IMD) support for radiosonde campaign at NARL. One of the authors, *Kalapureddy* is thankful to the DOS/ISRO for providing Research Fellowship during the period of the work. He is also grateful to Director, IITM for encouragement of this publication.

References

Anandan, V.K., Balamuralidhar, P., Rao, P.B., Jain, A.R., Pan, C.J., 2005. An adaptive moments estimation technique applied to MST radar echoes. Journal of Atmospheric and Oceanic Technology 22, 396–408.

Angevine, W.M., White, A.B., Avery, S.K., 1994. Boundary-layer depth and entrainment zone characterization with a boundary-layer profiler. Boundary-Layer Meteorology 68, 375–385.

Atlas, D., Srevastava, R.C., Sloss, P.W., 1968. Wind shear and reflectivity gradient effects on Doppler radar spectra, II. Journal of Applied Meteorology 8, 384–388.

Cohn, S.A., 1995. Radar measurement of turbulent eddy dissipation rate in the troposphere: a comparison of techniques. Journal of Atmospheric and Oceanic Technology 12, 85–95.

Doviak, R.J., Zrnic, D.S., 1984. Doppler Radar and Weather Observations. Academic Press, Orlando, FL, 458pp.

Ecklund, W.L., Carter, D.A., Balsley, B.B., 1988. A UHF wind profiler for the boundary-layer: brief description and initial results. Journal of Atmospheric and Oceanic Technology 5, 432–441.

Frisch, A.S., Clifford, S.F., 1974. A study of convection capped by a stable layer using Doppler radar and acoustic echo sounders. Journal of Atmospheric Science 31, 1622–1628.

Fukao, S., Yamanaka, M.D., Naoki, A.O., Hocking, W.K., Sato, T., Yamamoto, M., Nakamura, T., Tsuda, T., Kato, S., 1994. Seasonal variability of vertical eddy diffusivity in the middle atmosphere 1. Three-year observations by the middle and upper atmosphere radar. Journal Geophysical Research 99, 18,973–18,987.

Furumoto, J., Tsuda, T., 2001. Characterization of energy dissipation rate and effect of humidity on turbulence echo power revealed by MU radar RASS measurements. Journal of Atmospheric and Terrestrial Physics 61, 1123–1130.

Gage, K.S., 1990. Radar observations of the free atmosphere: structure and dynamics. In: Atlas, D. (Ed.), Radar in Meteorology. American Meteorological Society, Boston, pp. 534–565.

Gage, K.S., Balsley, B.B., 1978. Doppler radar probing of clear atmosphere. Bulletin American Meteorology Society 59, 1074–1093.

Ghosh, A.K., Jain, A.R., Sivakumar, V., 2003. A simultaneous MST radar and radiosonde measurements at Gadanki (13.5° N, 79.2° E) Part-II: determination of various turbulence parameters. Radio Science 38, 10.

Gossard, E.E., 1990. Radar research on the atmospheric boundary-layer. In: Atlas, D. (Ed.), Radar in Meteorology. American Meteorological Society, Boston, pp. 477–527.

Gossard, E.E., Strauch, R.G., 1983. Radar Observations of Clear Air and Clouds. Elsevier, Amsterdam, New York, 280pp.

Gossard, E.E., Wolfe, D.E., Moran, K.P., Paulus, R.A., Anderson, K.D., Rogers, L.T., 1998. Measurements of clear-air gradients and turbulence properties with radar wind profilers. Journal of Atmospheric and Oceanic Technology 15, 321–342.

Hashiguchi, H., Fukao, S., Tsuda, T., Yamanaka, M.D., Harijono, S.W.B., Wiryosumarto, H., 1996. An overview of the planetary boundary-layer observations over equatorial Indonesia with an L-band clear-air Doppler radar. Contributions to Atmospheric Physics (Beitr. Phys. Atmosph.) 69, 13–25.

Hermawan, E., Tsuda, T., 1999. Estimation of turbulence energy dissipation rate and vertical eddy diffusivity with MU radar RASS. Journal of Atmospheric and Terrestrial Physics 61, 1123–1130.

Hocking, W.K., 1983. On the extraction of atmospheric turbulence parameters from radar backscatter Doppler spectra I, Theory. Journal of Atmospheric and Terrestrial Physics 45, 89–102.

Hocking, W.K., 1985. Measurements of turbulent energy dissipation rates in the middle atmosphere by radar techniques: a review. Radio Science 20, 1403–1422.

Hocking, W.K., 1988. Two years of continuous measurements of turbulence parameters in the upper mesosphere and lower thermosphere made with a 2 MHz radar. Geophysical Research 93, 2475–2491.

Hocking, W.K., 1990. Turbulence in the region 80–120 km. Advanced Space Research 17, 37–47.

Hocking, W.K., Mu, K.L., 1997. Upper and middle tropospheric kinetic energy dissipation rates from measurements of C_n^2—review of the theories, in-situ investigations, and experimental studies using the Backland Park atmospheric radar in Australia. Journal of Atmospheric and Terrestrial Physics 59 (14), 1779–1803.

Jain, A.R., Jaya Rao, Y., Rao, P.B., Anandan, V.K., Damle, S.H., Balamuralidhar, P., Kulakerni, A., Viswanathan, G., 1995. Indian MST radar, 2. First scientific results in ST mode. Radio science 30, 1139–1158.

Joseph, P.V., Raman, P.L., 1966. Existence of low-level westerly jet-stream over peninsular India during July, Indian Journal of Meteorological. Geophysics 17, 437–471.

Joseph, P.V., Sijikumar, S., 2004. Intra seasonal Variability of the Low-Level Jet Stream of the Asian Summer Monsoon. Journal of Climate 17, 1449–1458.

Krishna Reddy, K., Kozu, T., Ohno, Y., Nakamura, K., Srinivasula, P., Anandan, V.K., Jain, A.R., Rao, P.B., Ranga

Rao, R., Viswanthan, G., Rao, D.N., 2001. Lower atmospheric wind profiler at Gadanki, Tropical India: initial result. Meterologische Zeitschrift 10, 457–466.

Madhu C. Reddy, K., Ghosh, A.K., Sivakumar, V., Jain, A.R., Kozu, T., Krishna Reddy, K., 2000. Integrated measurements of atmospheric winds using Indian MST radar and Lower Atmospheric Wind Profiler (LAWP)'. In: Proceedings of Ninth International Workshop on Technical and Scientific Aspects of MST Radar-MST combined with COST-76 final profiler workshop, 13–17 March 2000, Toulouse, France, pp. 222–225.

Narayana Rao, D., Kishore, P., Narayan Rao, T., Vijaya Bhaskara Rao, S., Krishna Reddy, K., Yarraiah, M., Hareesh, M., 1997. Studies on refractivity structure constant, eddy dissipation rate and momentum flux at a tropical latitude. Radio Science 32, 1375–1389.

Narayana Rao, D., Ratnam, M.V., Narayan Rao, T., Rao, S.V.B., 2001. Seasonal variation of vertical eddy diffusivity in the troposphere, lower stratosphere and mesosphere over a tropical station. Annals of Geophysics 19, 975–984.

Nastrom, G.D., 1997. Doppler radar spectral width broadening due to beam width and wind shear. Annals of Geophysics 15, 786–796.

Nastrom, G.D., Eaton, F.D., 1997. Turbulence eddy dissipation rates from radar observations at 5–20 km at White Sand Missile Range, New Mexico. Journal of Geophysical Research 102, 19,495–19,506.

Rao, P.B., Jain, A.R., Kishore, P., Balamuralidhar, P., Damle, S.H., Viswanathan, G., 1995. Indian MST radar 1. System description and sample vector wind measurements in ST mode. Radio Science 30, 1125–1138.

Riddle, A.C., 1983. Parameterization of spectrum. In: Bowhil, S.A., Edwards, B. (Ed.), MAP handbook, SCOSTEP Secr., Urbana,III., vol. 9, pp. 546–547.

Rogers, R.R., Ecklund, W.L., Carter, D.A., Gage, K.S., Ethier, S.A., 1993. Research applications of a boundary-layer wind profiler. Bulletin American Meteorology Society 74, 567–580.

Sandra Jocoby-Koaly, Campistron, B., Bernard, S., Blnech, B., Ardiiuin-Girard, F., Dessens, J., Dupont, E., Carissimo, B., 2002. Turbulent dissipation rate in the boundary-layer via uhf wind profiler Doppler spectral width measurements. Boundary-Layer Meteorology 103, 361–389.

Satheesan, K., Krishna Murthy, B.V., 2002. Turbulence parameters in the tropical troposphere and lower stratosphere. Journal Geophysical Research 107 (0).

Sato, T., Woodman, R.F., 1982. Fine altitude resolution observations of stratospheric turbulent layers by the Arecibo 430-MHz radar. Journal of Atmospheric Science 39, 2546–2552.

Sloss, P.W., Atlas, D., 1968. Wind shear and reflectivity gradient effects on Doppler radar spectra. Journal of Applied Meteorology 25, 1080–1089.

White, A.B., Lataitis, R.J., Lawrence, R.S., 1999. Space and time filtering of remotely sensed velocity turbulence. Journal of Atmospheric and Oceanic Technology 16, 1967–1972.

Woodman, R.F., 1985. Spectral moment estimation in MST radars. Radio Science 20 (6), 1185–1195.